

# Nature of the attractive interaction between proton acceptors and organic ring systems: Supporting Information

Emmanuel Arras,<sup>‡</sup> Ari Paavo Seitsonen,<sup>§</sup> Florian Klappenberger,<sup>\*,‡</sup> and Johannes  
V. Barth<sup>\*,‡</sup>

*Physik Department E20, Technische Universität München, James-Franck Straße, 85748  
Garching, Germany, and Physikalisch-Chemisches Institut der Universität Zürich,  
Winterthurerstr. 190, CH-8057 Zürich, Switzerland*

E-mail: florian.klappenberger@tum.de; jvb@ph.tum.de

Phone: +49 (0)89 289 12810. Fax: +49 (0)89 289 12338

---

\*To whom correspondence should be addressed

<sup>‡</sup>Physik Department E20, Technische Universität München, James-Franck Straße, 85748 Garching, Germany

<sup>§</sup>Physikalisch-Chemisches Institut der Universität Zürich, Winterthurerstr. 190, CH-8057 Zürich, Switzerland

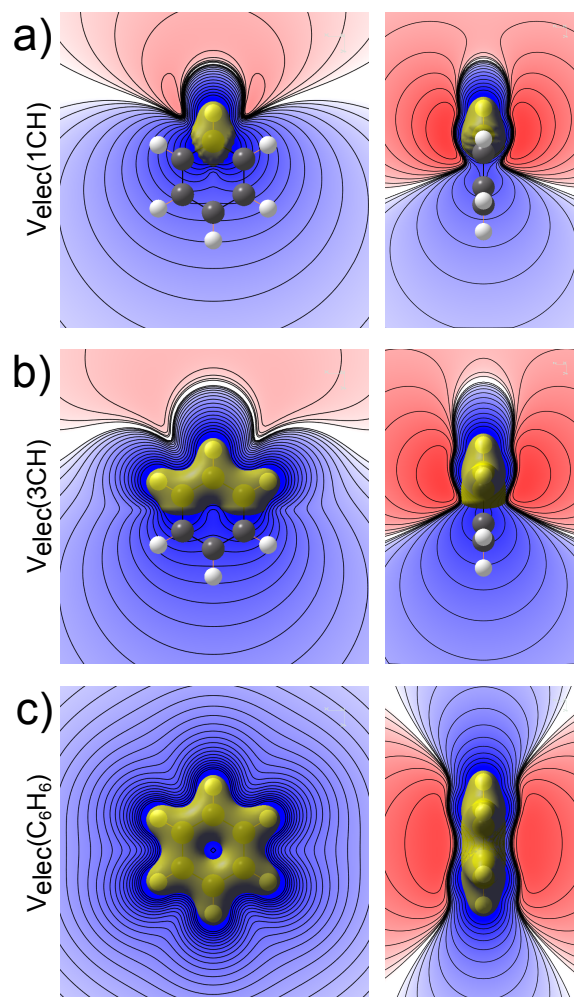


Fig. S1: Decomposition of the electrostatic potential into its contributing parts, in the case of the benzene ring. The total electron density of  $C_6H_6$  is first obtained via *ab initio* calculation. It is then cut symmetrically to get the partial densities (yellow isosurface) for the subunits 1CH and 3CH. A non-periodic poisson solver is applied to evaluate the corresponding electrostatic potentials  $V_{elec}$ . Red (blue) area indicates negative (positive) potential, *i.e.*, under the influence of a negative (positive) charge. a) Only one methine group is considered. The resulting potential clearly shows the contribution of a dipole, with a negative charge on the hydrogen side, and a positive charge on the carbon side. This directly contrasts the results of the standard Bader analysis. Furthermore, the side view indicates the presence of higher order multipoles. b) Half of the benzene ring is considered. The "inverse" dipole remains. c) The full benzene is taken into account. Now the positive potential prevails in the entire ring plane.

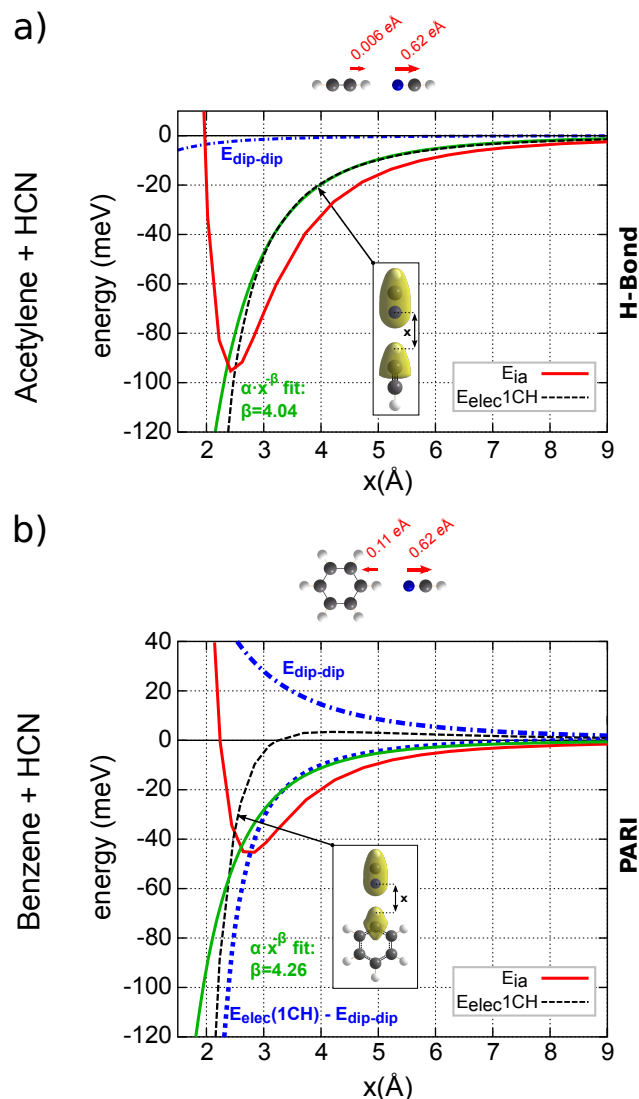


Fig. S2: Deconvolution of the electrostatic interaction energy of the highlighted CH unit,  $E_{elec}(1CH)$ , into the dipole-dipole related  $E_{dip-dip}$  and the residual part. The latter is fitted with a  $\alpha \cdot x^\beta$ -function, where  $\alpha$  and  $\beta$  are fit parameters. The interaction energy ( $E_{ia}$ , red line) is plotted for comparison. a) H-bond case: The exponent of the fit to the methine-related electrostatic energy ( $\beta = -4.04$ ) is typical of a dipole-quadrupole interaction. The dipole-dipole interaction energy is negligible because of the very weak dipole moment of the acetylene CH moiety. b) PARI-case: The repulsive dipole behaviour is consistent with long-range repulsion observed for  $E_{elec}(1CH)$ , the electrostatic part of the interaction energy originating from a single methine unit. The exponent for the  $E_{elec}(1CH) - E_{dip-dip}$  curve (blue dotted line) is  $\beta = 4.26$ , also typical of a dipole-quadrupole interaction to which presumably also a quadrupole-quadrupole interaction (power 5 exponent) contributes.

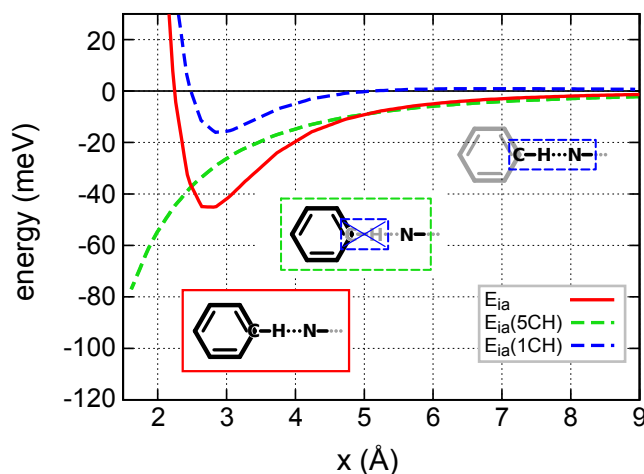


Fig. S3: Interaction energy  $E_{ia}$  (continuous red line) and its components as a function of the H...N distance in case of benzene-HCN complex.  $E_{ia}(5CH)$ , the dashed green curve, was calculated by taking into account only the electrostatic interaction originating from the non-adjacent methine groups, *i.e.*, the five CH units *not* being close to the N atom. Since the distances between the N atom and the atoms constituting to the non-adjacent part of benzene are larger than 4.1 Å the London dispersion and Pauli repulsion contributions are negligible. Therefore,  $E_{ia}(5CH)$  can be thought of as representing the interaction energy between the non-adjacent benzene part and HCN.  $E_{ia}(1CH)$ , the dashed blue curve, was calculated by subtracting  $E_{ia}(5CH)$  from  $E_{ia}$  and represents the interaction energy from the closest methine group comprising electrostatic, London dispersion and Pauli repulsion forces. We deduce from this result that the major part ( $\approx$  two third) of the interaction energy is originating from contributions of non-adjacent benzene moieties with only one third of the interaction originating from the closest methine group.

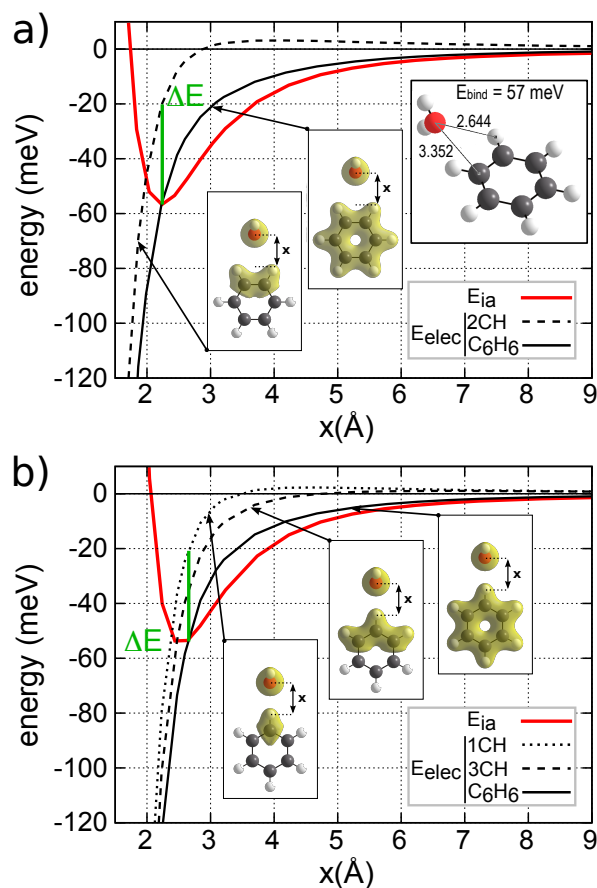


Fig. S4: Interaction energy in the benzene-water system as a function of the distance  $x$ . (a) When water is located *between* two methine groups (a 3D view with equilibrium bonding distances given in Å is shown in the inset) the interaction energy in the equilibrium position is slightly higher than in the case of water being in line with the CH axis of a single methine group (b). The general behavior is the same for both cases, *i.e.*, the electrostatic interaction with the nearby methine groups produces a slight repulsion at larger distances and the full electrostatic densities are necessary to describe the binding situation. At the equilibrium distance the electrostatic contribution of the benzene remote part,  $\Delta E$ , amounts to 30 – 40 meV in either situation.

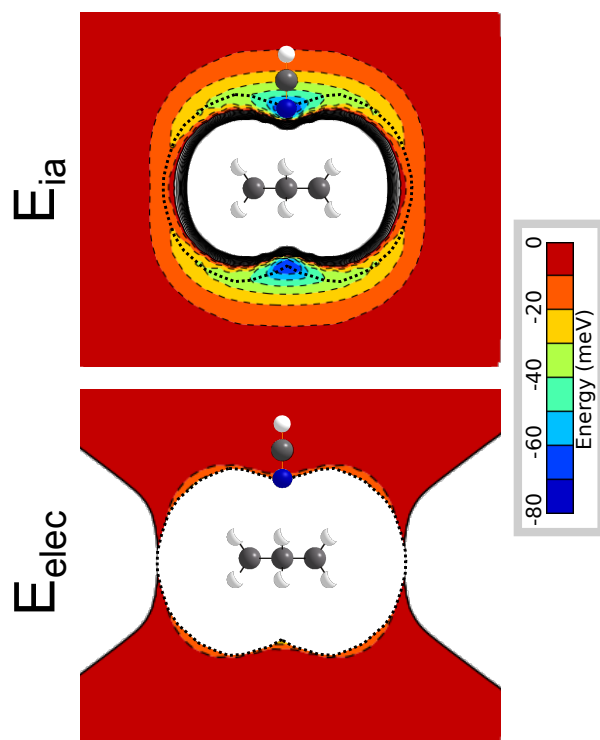


Fig. S5: The interaction of HCN with an artificially flat configuration of cyclohexane ( $C_6H_{12}$ ), which is used as a model of a flat ring systems containing only  $\sigma$  bonds. The planar geometry of the carbon ring is not the energy minimum conformation for cyclohexane, therefore the MP2-calculated energetics of the interaction might not reach the same accuracy as for the other cases of this study. Nevertheless, the employed flat geometry is advantageous because it allows a direct comparison with the other planar cases of PARI. The full interaction energy as calculated *ab initio* is shown in the upper panel, and the electrostatic part of it is displayed in the lower panel. One can see the attractive regime all around the  $C_6H_{12}$ , along with its dispersive origin, as electrostatic interactions are extremely weak. Furthermore, the electrostatic contribution does not lead to attraction within the plane defined by the ring in marked contrast to all other ring system studied here, that contained at least one  $\pi$  bond.

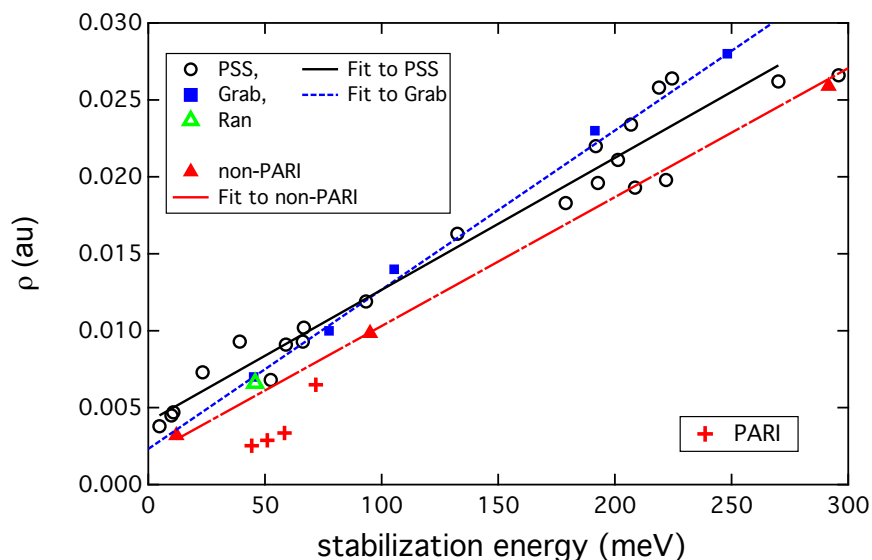


Fig. S6: Graph of the correlation between the electron density  $\rho$  (in atomic units) at the bond critical point ( $H \cdots A$ ) and the stabilization energy (in meV) for the different bimolecular complexes. For hydrogen bonding situations the work of Grabowski (Grab, blue squares, Ref. 1), Parthasarathi, *et al.* (PSS, black circles, Ref. 2), Ran, *et al.* (Ran, open green triangle, Ref. 3), and our own test calculations for typical hydrogen bonding situations (non-PARI, red full triangles) agree on a linear correlation. In contrast, the PARI cases of this work (PARI, red crosses), which are cyclopentadiene $\cdots$ NCH, Bz $\cdots$ NCH, Bz $\cdots$ H<sub>2</sub>O, and NC<sub>5</sub>H<sub>5</sub> $\cdots$ NCH in order of increasing stabilization energy, are clearly offset from this correlation. In the PARI situation a certain complex stabilization energy is achieved with a much lower electron density than for hydrogen bridges of the same strengths.

## References

- 1 S. J. Grabowski, *Chem. Phys. Lett.*, 2001, **338**, 361–366.
- 2 R. Parthasarathi, V. Subramanian and N. Sathyamurthy, *J. Phys. Chem. A*, 2006, **110**, 3349–3351.
- 3 J. Ran and M. W. Wong, *J. Phys. Chem. A*, 2006, **110**, 9702–9709.